RSC Advances

ROYAL SOCIETY OF CHEMISTRY

www.rsc.org/advances

RSC Advances

ARTICLE

Synthesis of hexagonal mesoporous silicates with amino groups functionalized on the pore channels by a co-condensation approach

Received 00th January 20xx,
Accepted 00th January 20xx

DOI: 10.1039/x0xx00000x

www.rsc.org/advances

Yunping Li,[ab‡] Wei Xiong,[ab‡] Chun Wang,[a]* Bo Song[ac] and Guolin Zhang[a]

Mesoporous silicates with amino groups functionalized on the pore channels have been made by co-condensation of tetraethoxyl siloxide (**TEOS)** with precursors of **P-Si** through a triblock copolymer-templated sol-gel proess under acidic comdition. Poly(alkylene oxide) block copolymer(**P123**) was eluted by ethanol extraction and template molicules were removed by refluxing the materials in a mixture of DMSO and water. The resulted materials were characterized in detail by means of FT-IR, XRD, TEM and N_2 adsorption, in order to study the effect of precursors on their mesoscopic order and pore structure. Evidence of amino groups located on the pore channels was found through variation of pore size and BET surface after amino groups coupled with benzaldehyde and TEM images of materials after stained by RuO_4. Finally, comparative study on catalytic performance of materials SBA-**Am**-10 and SBA-**T**-10, obtained by two methods revealed that catalyst synthesized by our method gave rapid speed and higher yield to flavanone from Claisen-Schmidt condensation of benzaldehyde and 2′-hydroxyacetphenone.

1 Introduction

Amino-functionalized mesoporous materials have received considerable attention in recent years among the variety of organo-functionalized mesoporous materials synthesized through the direct synthesis route. It has been found to be effective in base catalyzed reactions[1-5] or further post-synthesis functionalization.[6,7] However, most of the work was on the modification of small mesopores of MCM-type,[8] which were synthesized under basic conditions. Highly ordered mesoporous materials with large pores (>4.5 nm) have recently attracted particular interest from catalytical view. The large pore diameters of the channels facilitate the molecular diffusion and accessible to catalytical sites and improve the catalytical efficiency. On the other hand, the well-defined channels also have confined effect on the catalytic selectivity. In several investigations, confinement of the catalyst in the mesoporous solid improved the activity compared to attachment to amorphous[9] or microporous silica,[10] due to enhanced selectivity in a steric homogeneous environment. It is generally admitted that antagonistic effects at the mesoscale result in the existence of an optimal catalytic efficiency depending on pore size.[11]

However, well-ordered large pore amino-functionalized mesoporous materials are perhaps the most difficult to synthesis using a direct synthesis approach in the presence of non-ionic surfactants as structure directing agents under acidic condition. Prehydrolysis method probably was the most efficient approach to obtain well-ordered materials, in which the silica source, usually **TEOS** or sodium silicate (Na_2SiO_3), were pre-hydrolysed for certain time before the functional monomers were added. In order to gain well-ordered mesoporous structure, the optimal prehydrolysis time of **TEOS** was 2 h.[12] In this case, an intact silicate framework was formed before the addition of (3-aminopropyl)triethoxysilane (**APTES**), which could minimize the effect of the protonated amino groups on the self-organization of the surfactants. Protonated species can cross-link with the alkoxysilane precursor during the condensation step and as a consequence the organosilanes are eventually deposited both in the pore channels and inside the walls of the mesoporous materials.[13] As a result, amino groups were buried in the silica matrix and on both inner and outer surfaces of the mesopores.[14] This is not desired in point of confined catalysis. Another commonly adapted method to obtain ordered amino-functionalized mesoporous silicates was to use inorganic salts as additives to strengthen the intereaction between the silicate species and the surfactant hydrophilic head groups.[15] However, the accessibility of the amino groups in the resulted material was remained unknown.

In our previous research to prepare molecular imprinted mesoporous silicates (**MIMS**) for 2-naphthol by a surfactant directed sol-gel process, we found that instead of imprinting the template in the matrix, the material turned out to be a periodic mesoporous silicate with inner amino functionalized mesoporous pores.[16] We rationalized that this was due to the mono-functionalized organic template tends to interact with the

[a] Chengdu Institute of Biology, Chinese Academy of Sciences, Chengdu 610041, China. E-mail: wangchun@cib.ac.cn
[b] University of Chinese Academy of Sciences, Beijing 100049, China
[c] College of Architecture and Environment, Sichuan University, Chengdu 610065, China
‡ These authors contributed equally to this work.
† Footnotes relating to the title and/or authors should appear here.
Electronic Supplementary Information (ESI) available: [details of any supplementary information available should be included here]. See DOI: 10.1039/x0xx00000x

hydrophobic core of the surfactant micelle during sol-gel process. This enlightened us to use aromatic groups as protecting groups for amino in order to obtain well-ordered inner pore amino functionalized mesoporous materials.

Synthesis of functionalized mesoporous materials through protecting group strategies were used by several research groups. Schuths groups synthesized cyano (-CN) functionalized SBA-15 and further hydrolysed into carboxyl (-COOH).[17] Corrius groups reported the use of N-tert-butyloxycarbamate (-Boc) as protecting group for preparation of amino functionalized SBA-15.[18] Despite the difficulty in preparing Boc-protected monomers, the ordering of the resulted mesoporous materials were poorly preserved.

The structure and contents of organo-functionalized mesoporous materials synthesized from co-condensation of **TEOS** and functional monomer in the presence of surfactant, depends strongly on the nature of the functional monomers. In fact, the strong hydrophobic interaction between phenyl groups and the hydrophobic core of the pluronic type surfactants was theoretical investigated by A. Patti et al. using lattice Monte Carlo simulations. They observed when the hybrid precursor was sufficiently hydrophobic, it could act as a co-surfactant, swell the core of the surfactant liquid crystal, and lead to structures with smaller interfacial curvature. On the other hand, if the hybrid precursor acted as a co-solvent it would solubilize the surfactant leading to the destruction of the preformed liquid crystal.[19] We visualize that is possible to obtain highly ordered organo-functionalized mesoporous materials with accessible organic groups on the pore channels, by carefully selecting functional monomers with suitable solubility and hydrophobicity.

In this paper, we reported the synthesis of amino-functionalized mesoporous material with several aromatic groups as protecting groups, and compared with materials synthesized by pre-hydrolysis method. The major features of this work are comparison of products from both methods with respect to efficiencies of the synthetic routes, precursor effects, the locations of functional groups in the mesoporous products, and the catalytical behaviors in solid state catalyzed synthesis of flavanone.

2 Experimental

2.1 Chemicals and Materials

Phenol (**Ph**), 2-naphthol (**Np**), 4-benzylphenol (**Bp**), 9-anthracenemethanol (**Am**), di-tert-butyl dicarbonate (**DbD**) and **TEOS** were purchased from Gracia Chemical Technology Co., Ltd. Chengdu. 3-isocyanatopropyltriethoxysilane (**IPTES**), **APTES** and Pluronic P123 ($EO_{20}PO_{70}EO_{20}$, MW= 5800 Da) were purchased from Sigma Chemical Co., St. Louis. All other

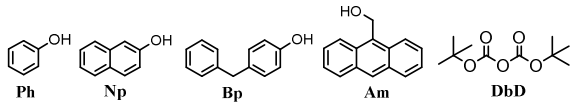

chemicals used were of analytical grade. All solvents and reagents were used without further purification except THF (dried).

2.2 Instrumentation

The infrared spectra were recorded with Perkin-Elmer system 2000 FT-IR spectrometer. Transmission electron microscopy (TEM) images were obtained on a Tecnai-G2-F20 electron microscope operating at 200 kV. X-Ray diffraction (XRD) patterns were obtained at room temperature using instrument equipped with a Cu kα X-ray source. The content of total amino groups in the samples was determined by the CHN elemental analysis, which was performed using a PerkinElmer 2400 Elemental Analyzer. Solid-state cross-polarization (CP) magic-angel spinning (MAS) nuclear magnetic resonance (NMR) analysis was carried out on a Bruker AV-400 spectrometer at 79.49 MHz for ^{29}Si and 100.61 MHz for ^{13}C. The ^{29}Si MAS NMR spectra were measured at 60 s repetition delay and 3 μs pulse width. The ^{13}C CP MAS NMR spectra were measured at 2 s repetition delay, 2 ms contact time and 2.8 μs ^{1}H 90° pulse. All chemical shifts were referenced to tetramethylsilane (TMS). Nitrogen adsorption-desorption isotherms were measured at 77K using a HYA2010-B2 system. The Barret-Joyner-Halenda (BJH) pore size distribution was calculated from the desorption branch of the isotherm.

2.3 Synthesis of materials

The synthesis of aromatic protecting triethoxysilane precursors (**APTP**s) was achieved referring to the method in ref 20. Aromatic moieties (**Ph**, **Np**, **Bp**, **Am**) were reacted with stoichiometric amount of **IPTES** using triethylamine as catalyst in dried THF at 65°C until the reaction was totally carried out. The products were obtained by evaporation of solvents and purified by column chromatography. The products synthesized with **Ph**, **Np**, **Bp**, **Am** were identified as **Ph-Si**, **Np-Si**, **Bp-Si**, **Am-Si** respectively. For comparison, **Boc** protecting triethoxysilane precursor synthesized by **DbD** was obtained according to the method in ref 18 and named as **Boc-Si**.

Amino-functionalized SBA-**P**-x materials were synthesized by following procedure:

Throughout this paper, we abbreviate the amino-functionalized mesoporous silica materials as SBA-**P**-x or SBA-**T**-x (where **P** is **Ph**, **Np**, **Bp**, **Am** or **Boc**, **T** denotes **APTES** and x is 3, 5, 7, 10, 15 or 20, which is calculated from the molar percentage of [precursor/(precursor + TEOS)]. **P-Si** denotes triethoxysilane precursors and x denotes the molar percentage of **P-Si** or **APTES** in the total silane monomer used in the co-condensation reaction.

P-Si functionalized SBA-15 material was synthesized under acidic conditions from a P123/**TEOS**/**P-Si**/HCl/H_2O mixture with a molar composition of 0.0172/1/x%/6/208. Typically, P123 (2.0 g) was fully dissolved in 75 ml of 1.6 M HCl. To the solution was added a stoichiometric amount of **P-Si**, which was pre-dissolved by 1 ml THF. After the pre-hydrolysis of **P-Si**, **TEOS** (4.45 ml) was added to the mixture and stirred up to 24 h at 40°C. Then the mixture was transferred into an autoclave aging at 100°C for 24 h. After cooling down to room temperature, the resultant particles were isolated by filtration and rinsed with water, and named as SBA-**P**-x-as. P123 was extracted by Soxhlet extraction with ethanol for 24 h, the materials with P123 removed was designated as SBA-**P**-x-PR.

By refluxing the particles in a mixture of DMSO and water (v/v, 40/1) at 160°C for 6 h, the carbamate bond was cleaved and **P** was removed, except that **Boc** was removed by acidic hydrolysis. After filtration, the materials were rinsed with DMSO and ethanol successively, and vacuum dried at 60°C for 24 h. The pre-hydrolysis time of **P-Si** were 1.5 h. Pure SBA-15 was prepared by the similar way without functional group adding. For comparison, SBA-**T**-x was synthesized by adding **APTES** after 2 h pre-hydrolysis of **TEOS**.

2.4 Chemical component, texture and structural characterizations

The nitrogen content, corresponding to the amino groups incorporated, was measured by elementary analysis. Texture properties were determined from N_2 adsorption/desorption and the specific surface areas were evaluated by the Brunauer-Emmett-Teller (BET) method, pore size distribution profiles were calculated on the desorption branch of the isotherms using the Barrett-Joyner-Halenda (BJH) method. Information about mesoscopic order can be obtained by TEM and crystallographic form can be observed by small angel X-ray diffraction (SXRD) approach.

2.5 Determination of the location of aminopropyl groups

2.5.1 Condensation reaction of the amine groups with benzaldehyde

Two kinds of solid amino functionalized SBA-15 (SBA-**Am**-10, 0.25 g and SBA-**T**-10, 0.25 g) were dispersed in anhydrous toluene, an excess of benzaldehyde (2 equiv. of benzaldehyde per NH_2 moiety) and 100 µl glacial acetic acid was added. The reaction was carried out under reflux for 12 h, then the resulted materials, denoted as SBA-**Am**-imine and SBA-**T**-imine, were filtered and wash with adequate toluene and ethanol to eliminate the unreacted benzaldehyde, after dried at 80°C for 6 h，the changes of pore diameters, BET surfaces and pore volumes were determined by nitrogen adsorption measurements.

2.5.2 Characterization by combination of staining technique and TEM

Following a general method[14] for RuO_4 staining SBA-15, SBA-**Am**-10 and SBA-**T**-10 have been exposed to the vapor of 0.5 % RuO_4 (aq.) for 15 min to stain amino groups. Then the stained samples were characterized by Transmission electron micrographs on a Tecnai-G2-F20 electron microscope working at 200 kV.

2.6 Catalytic reaction

In order to remove the residue Cl^- ions and to neutralize the protonated amine groups, the functionalized SBA-15 materials were dispersed into 100 ml of 0.1 M methanol solution of TMAOH at room temperature for 40 min before the reactions. The resulted solids were recovered by filtration, washed with methanol, and finally dried at 100°C for 12 h.

2.6.1 Kinetic study of flavanone synthesis catalyzed by SBA-T-10 and SBA-Am-10

Two kinds of amine functionalized SBA-15 (SBA-**T**-10 and SBA-**Am**-10) were selected for kinetic study, the reaction was carried out in a two necked flask equipped with a reflux condenser and a magnetic stir bar. Typically, 6 mmol (612 µL) benzaldehyde (**A**) and 4 mmol (485 µL) 2'-hydroxyacetophenone (**B**) were stirred in 25 ml DMSO, 250 mg of SBA-**T**-10 (or SBA-**Am**-10) was added into the solution. The mixture was heated to 140 °C under stirring for 14 h. To get the kinetic curve, the reaction was monitored every two hours by withdrawing an aliquot of solution from the flask. The samples were filtered and the filtrates were analyzed using an Agilent HPLC equipped with an Agilent C18 column (4.6 × 250 mm, 5 µm) to determine the yields of flavanone (**Fl**).

2.6.2 Intramolecular Michael addition of 2'-hydroxychalcone catalyzed by SBA-T-10 and SBA-Am-10

The reaction was carried out in a round-bottom flask equipped with a reflux condenser and a magnetic stir bar. Typically, 20 mg SBA-**T**-10 (or SBA-**Am**-10) was suspended in 2.0 ml DMSO, 0.036 mmol (8.0mg) 2'-hydroxychalcone (**Ch**) was added into the suspension. The mixture was heated to 140 °C under stirred for 4h. After cooling to room temperature, the mixture was filtered and the filtrate was analysed by ^{1}H NMR. The conversion of **Ch** and the yield of **Fl** were calculated from the relative volume of C2-H on **Fl** and β-H of the carbonyl on **Ch**. Control experiments were conducted in the presence of blank SBA-15, with and without DMSO, or without added solvent and catalyst under otherwise same conditions as described above. Each reaction was repeated for tree times and the average analysed volume vs time was plotted in Fig. 6.

3 Results and discussion

3.1 Synthesis of materials

The aryl protected functional monomers were synthesized according to published procedure.[20] Aromatic hydroxyl moieties were reacted with a stoichiometric amount of **IPTES**, respectively, using triethylamine as catalyst in dried THF at 65°C for 24 h. The products were obtained by evaporation of solvents, and identified as **P-Si** (Scheme 1, a)). For comparison, **Boc** protected functional monomer (**Boc-Si**) was prepared by following Cprriu et al's method (Scheme 1, b)).[18]

The amino-functionalized mesoporous materials (SBA-**P**-x) were prepared by a co-condensation of trialkoxysilanes (**P-Si**) and **TEOS** through a triblock copolymer-templated sol-gel process[16] with a slight modification. **P-Si** was added into the surfactant/HCl solution and allowed to pre-hydrolysis for 1.5 h before addition of **TEOS**, to let the aromatic groups fully interacted with the surfactants micelle. Surfactant was

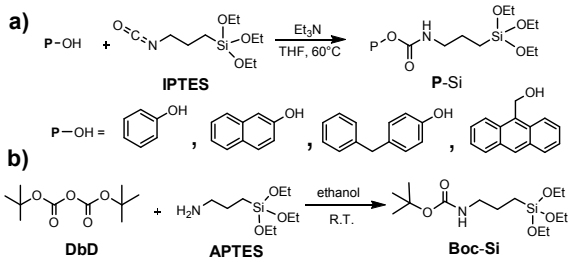

Scheme 1 Synthesis of the aryl protected functional monomers.

removed by ethanol extraction. To remove the aromatic protecting groups (**P**), the carbamate bond was cleaved by heating the materials in DMSO/H_2O at 160°C, while the one synthesized by **Boc-Si** was heated in aqueous solution of HCl. After filtration and dried at 60°C for 24 h, a series of amino functionalized materials can be obtained.

SBA-**T**-x were synthesized by adding **APTES** after 2 h pre-hydrolysis of **TEOS**.[12] The surfactant was removed via the same way as SBA-**P**-x, then, the materials were dried at 60°C for 24 h for the further analysis.

3.2 FT-IR characterization

In order to confirm that the **P-Si** was incorporated in the structure and the successful cleavage of the carbamate bond, the directly synthesized material (SBA-**Am**-10-as), after surfactant removal (SBA-**Am**-10-PR) and after protecting group removal (SBA-**Am**-10) were characterized by Fourier transform infrared spectroscopy (FT-IR, Fig. 1). In all three materials, the clear bands around 1070 and 1220 cm^{-1} indicate that condensed silica networks are formed (Si-O-Si, asymmetric vibration). For the SBA-**Am**-10-as, absorbance peaks corresponding to C-H stretching and C-H deformation vibrations appear in the range of 2850-2900 cm^{-1} , which were due to CH_2 absorption of P123. This peak is reduced on SBA-**Am**-10-PR, indicating that the surfactant was almost removed upon extraction with ethanol. The characteristic bands of carbamate C=O stretching vibration around 1710 cm^{-1} are clearly visible for SBA-**Am**-10-as and SBA-**Am**-10-PR, indicating the existence of **P-Si**. After ethanol extraction and DMSO treatment, the 1710 cm^{-1} peak is disappeared (Fig.1, SBA-**Am**-10), indicating the cleavage of carbamate. An increasing intensity of the peak around 1640 cm^{-1} could be assigned to NH_2 bending, which was overlapped with an OH bending of absorbed water.[21]The relatively weak peak at 1503 cm^{-1} corresponding to the symmetric $–NH_3^+$ bending,[22] further proves the successful recovering of the amino groups from removal of the protecting group.

3.3 ^{13}C and ^{29}Si CP MAS NMR

The incorporation of amino moieties in the mesoporous materials was confirmed by solid-state NMR spectroscopy. The ^{13}C CP MAS NMR spectrum of SBA-Am-10-PR (Fig. 2a) demonstrates that Am-Si precursor was incorporated as shown by the signals at 56.7 ppm of CH_2, 157.1 ppm of carbamate C=O resonances, 124.2-132.6 ppm of anthracene ring and three additional signals (42.2, 21.3 and 9.1 ppm) are attributed to the propyl spacer of Am-Si. The remove of protecting group by the treatment of DMSO/H_2O is clearly reflected in Fig. 2b by the disappearance of signals (56.7, 157.1 and 124.2-132.6 ppm) while the signals (42.7, 21.5 and 9.3 ppm) of the propyl spacer were retained. The ^{29}Si MAS NMR spectrum of SBA-Am-10 (Fig. 3) exhibits two sets of signals attributed to T (C-SiO_3, -55 to -68 ppm) and Q (SiO_4, -90 to -120 ppm) environments. The presence of T units gives further evidence of the existence of CH_2-Si groups. These data could further support the conclusion that aminopropyl moieties were successfully incorporated into the mesoporous material SBA-Am-10 and the protecting groups were successfully removed.

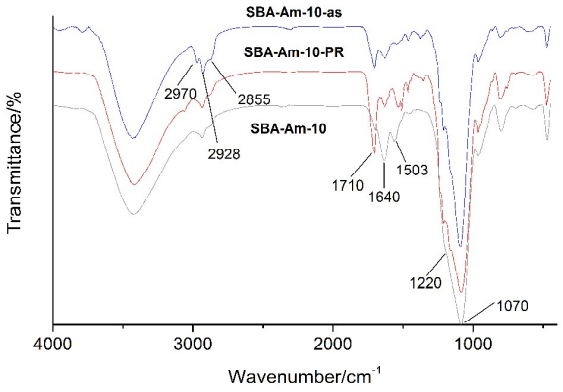

Fig. 1 FT-IR spectra of SBA-**Am**-10-as, SBA-**Am**-10-PR and SBA-**Am**-10.

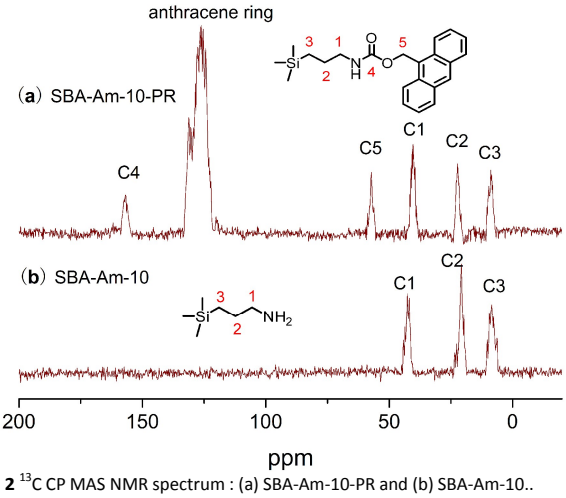

Fig. 2 ^{13}C CP MAS NMR spectrum : (a) SBA-Am-10-PR and (b) SBA-Am-10..

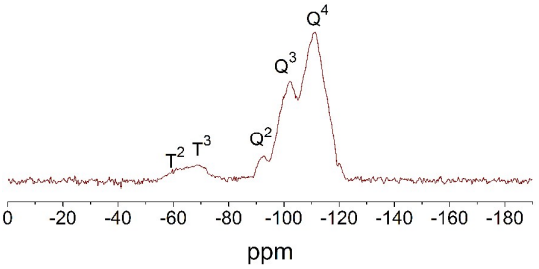

Fig.3 ^{29}Si MAS NMR spectrum of SBA-Am-10.

3.4 Elemental analysis

To further confirm the incorporation of aminopropyl groups, the N contents of the samples were analyzed by elementary analysis. The results were represented in Table 1. Percentages of functional monomer used and integrated, indicate that 81% to 89% of added functional monomers were integrated in the final materials. We also found that the time of functional monomer pre-hydrolysis would significantly affect the N content in the final materials (Data not shown in Table 1). The optimal pre-hydrolysis time was between 1 and 1.5 h. When pre-hydrolysis time was less than 1 h, only 6-7% of functional monomers were contained, prolonging hydrolysis time greater

than 1.5 h mwould not increase the functional monomer and resulted in less ordered materials.

3.5 Small angel X-ray diffraction measurements

The SXRD patterns of materials prepared from different precursors, SBA-**P**-10 (**P**=**Ph**, **Bp**, **Np**, **Am**, **T**) were represented in Fig. 4(a) and the effect of amount of aminopropyl contents from 5-20% were demonstrated by SBA-**Am**-X (X=5-20%, Fig. 3(b)). The SXRD patterns of materials in Fig. 4 (a) all show an intense peak of d (100) and two weak peaks of d (110) and d (200), which are characteristics of a 2-d hexagonally ordered (*p6mm*) structure.[23-25] However, all the amino functionalized materials were with lower ordering than the blank SBA-15, which could be attributed to the disturbance of the organic precursors to the ionic interaction between the silicate species and the surfactant hydrophilic head groups.

The structural ordering is very sensitive to the aromatic groups used in the aromatic group protected precursor **P-Si** and the way **P-Si** and **TEOS** are mixed. Well-ordered hexagonal mesoporous materials can be obtained with amino contents up to 20% for SBA-**Np**-x and SBA-**Am**-x (Only the later set is shown in Fig. 4 (b)). The intensity of the reflection declined as the proportion of functional monomer (x) increasing, suggesting that less ordered materials were resulted. However, for materials prepared with **Bp-Si** and **Ph-Si**, the long rang ordering were lost when x reached 10%. The peak intensity attributed to d 100 reflection was decreased with the order: SBA-**Np**-10>SBA-**Am**-10->SBA-**Bp**-10>-SBA-**T**-10>SBA-**Ph**-10.

When **P-Si** was pre-mixed with **TEOS** before being added into the surfactant solution as usual doing,[26] the resulting materials were amorphous. However, when **P-Si** was added into the surfactant solution 1 h earlier than **TEOS**, well ordered hexagonal structures were formed.

The varying intensity of d (100) in Fig. 4 (a) may be due to different interaction strengths between non-polar aromatic groups and the hydrophobic core of the surfactant micelle, which depends on the solubility, size and rigidity of the aromatic moieties.[19]When such hydrophobic interaction is strong enough, it would draw the organic precursors further into the micelles, leading to the formation of well-ordered mesopores (In the case of **Np-Si** and **Am-Si**), otherwise, resulting in disordered mesopores (In the case of **Bp-Si** and **Ph-Si**). The addition of organoalkoxysilane prior to **TEOS** into the surfactant solution would favor the interaction between the terminal organic moiety of the organoalkoxysilane and the core of the surfactant, therefore promote the formation of well-ordered meso-structures. Although pre-hydrolysis of **TEOS** can also get well-ordered mesoporous silicates by formation of an intact silica framework, which could shell the disruptive interactions of organic monomers with the micelles, but consequently the organic monomers were distributed in the silica walls. The reduced intensity of the d100 peak of SBA-**Am**-10 relative to SBA-**T**-10 (Fig. 4 (a), could be due to the organic content present in the pores.

It is worth to mention that with **Boc-Si** as precursor, no ordered material was obtained.

Table 1 Amino contents incorporated calculated from elementary analysis

Samples	N content (%)	Amino group (mmol g-1)	Percentage of functional precursor	
			used[a]	integrated[b]
SBA-Np-10	1.36	0.97	10%	8.2%
SBA-Am-10	1.46	1.04	10%	8.8%
SBA-Bp-10	1.34	0.96	10%	8.3%
SBA-Ph-10	1.31	0.93	10%	8.1%
SBA-T-10	1.47	1.05	10%	8.9%
SBA-15	—	—	—	—

[a] Molar ratio of P-Si/TEOS as added; [b] Molar ratio of P/SiO2 calculated from the N contents of elementary analysis.

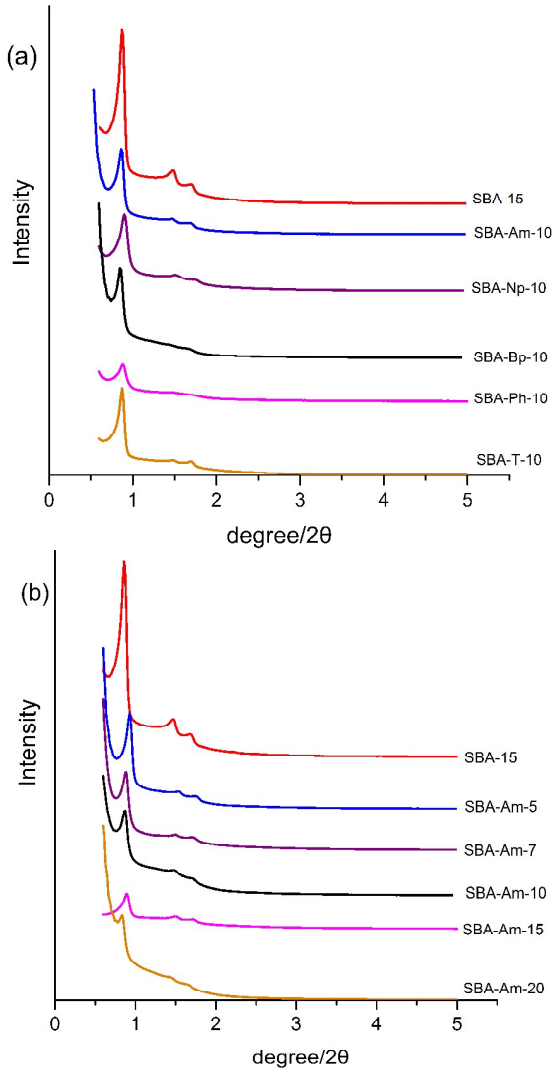

Fig. 4 XRD patterns of prepared materials a) SBA-**P**-5, P=**Am**, **Np**, **Bp** and **Ph** with different **APTPs** addition, b) SBA-**Am**-x with different concentrations of **Am-Si**.

3.6 Nitrogen adsorption/desorption characterization

Nitrogen adsorption/desorption isotherms of all obtained materials except SBA-**Ph**-10 (Fig 5 (a)), exhibited typical type IV isotherms according to IUPAC classification.[27] The Brunauer-Emmett-Teller (BET) surface area, pore size, and pore volume

Table 2 Texture data of the amine-functionalized SBA-15 prepared from different protecting groups and by pre-hydrolysis

Sample	Nitrogen Adsorption		
	Pore size (nm)	SBET (m2/g)	Pore volume (cc/g)
SBA-Np-10	7.16	439.625	0.945411
SBA-Am-10	6.58	571.566	0.941257
SBA-Bp-10	6.10	422.182	0.446348
SBA-Ph-10	4.22	498.411	0.464072
SBA-T-10	5.58	545.577	0.760954
SBA-15	6.56	689.486	1.096177

are listed in Table 2. The pore sizes of SBA-**Bp**-10 and SBA-**Ph**-10 were smaller than the blank SBA-15, probably due to the co-solvents effects of Bp and Ph to the surfactant. On the other hand, the pore sizes of SBA-**Np**-10 and SBA-**Am**-10 were larger than SBA-15, due to the strong interactions between these aromatic groups and the hydrophobic cores of the surfactants (co-surfactants effects), causing the swelling of the hydrophobic cores. Pore size distributions calculated from desorption branch of nitrogen adsorption isotherm are presented in Fig. 5 (b). Fig 5 (a) depicts that pure silica and SBA-**Np**-10, SBA-**Am**-10 show similar high porosity and well-defined adsorption. The sharp steep increases in the adsorption at P/P_0 = 0.7-0.8 implied that the materials of SBA-**Np**-10 and SBA-**Am**-10 possess large pore sizes with narrow distribution. This was conformed further by pore size distribution (Fig. 5 (b)). SBA-T-10 shows a less well-defined hysteresis loop than SBA-Np-10 and SBA-**Am**-10, SBA-**Bp**-10 and SBA-**Ph**-10 display poorer defined capillary condensation steps and lower porosity (Table 2, pore volume). SBA-**Bp**-10 and SBA-**Ph**-10 lose mesoporosity might result from the incorporated micelles being more poorly ordered. The decrease in surface area of SBA-**Np**-10 and SBA-**Am**-10 comparing with SBA-15 (Table 2), probably due to the strong interactions between the aromatic groups in the hydrophobic-hydrophilic palisade region of surfactant micelle, which could prevent the hydrophilic head of the surfactants reaching into the pore walls to form micropores.

The pore size of materials made with different aromatic protecting groups are in the order: SBA-**Np**-10>SBA-**Am**-10>SBA-**T**-10.

3.7 Transmission electron microscopy (TEM)

The mesoscopic order and symmetry inferred from XRD data can be further confirmed by TEM (Fig. 6). As can been seen, all materials except SBA-Ph-10 (not shown), show excellent hexagonal ordering of mesopores in a uniform longitudinal pore channel, characteristic of SBA-15 materials

The distributions of amino groups of materials made from TEOS prehydrolysis method (SBA-**T**-10) and through aromatic protecting group path (SBA-**Am**-10), were demnstrated by the selective complexation of RuO_4 over amino groups and its subsequent reduction to RuO_2. The sample treatment was similar with the method reported by Rual Sanz. [14] The high electronic density of this heavy metal makes the electron beam pass through it difficult when the sample is analysed by TEM. Thus, a specific darkening can be assigned to RuO_2 and, as a consequence, to the position of amino groups in the

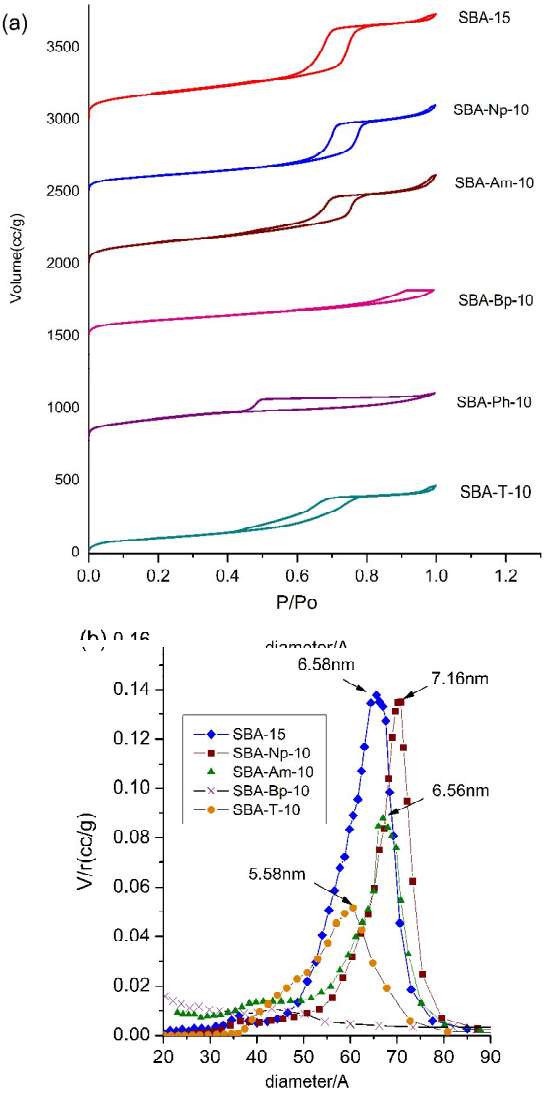

Fig. 5 (a) Nitrogen adsorption/desorption isotherms of SBA-**P**-10, (b) BJH pore size distribution of SBA-**P**-10.

samples.

The possible interaction of silanol groups of pure non-functionalized SBA-15 silica with the staining agent was checked for control. In order to giving a better view of the details, we enlarged the magnification of TEM images for stained SBA-15, SBA-**Am**-10 and SBA-**T**-10. (Fig. 6 (a'), (d') and (e')). Fig. 6(a) and (a') show the TEM micrographs for SBA-15 before and after the staining treatment with RuO_4. As can be seen, the bright and dark regions corresponding to pore cavities and pore walls, respectively. The contrasts are the same in both cases, that is, bright and dark areas correspond to the same regions (pore cavities and pore walls respectively) regardless of the treatment of RuO_4. The results indicate that RuO_4 does not interact with the silanol groups of the silica surface under the staining conditions used in this work.

TEM image of the stained SBA-**T**-10 (Fig. 6 (e') exhibits a number of black spots across the walls, assigned to ruthenium species fixed over amino groups homogeneously distributed in

the sample, including pores and walls. This was not the case of SBA-**Am**-10 (Fig. 6 (d')).. The dark areas of RuO_2 were mainly found within the channels for the stained sample, while the pore walls remained bright. This could be an evidence of amino groups located mostly on the pore surfaces of the nesosilicates. It is also clear that the amino-functionalized samples of SBA-**Am**-10 and SBA-**T**-10 present a distribution of pore cavities (bright) and pore walls (dark) similar to the silica SBA-15 before staining with RuO_4 (Fig. 6 (a), (d), and (e)). This could be an evidence that amino groups are not detectable by TEM if the staining step is not performed.

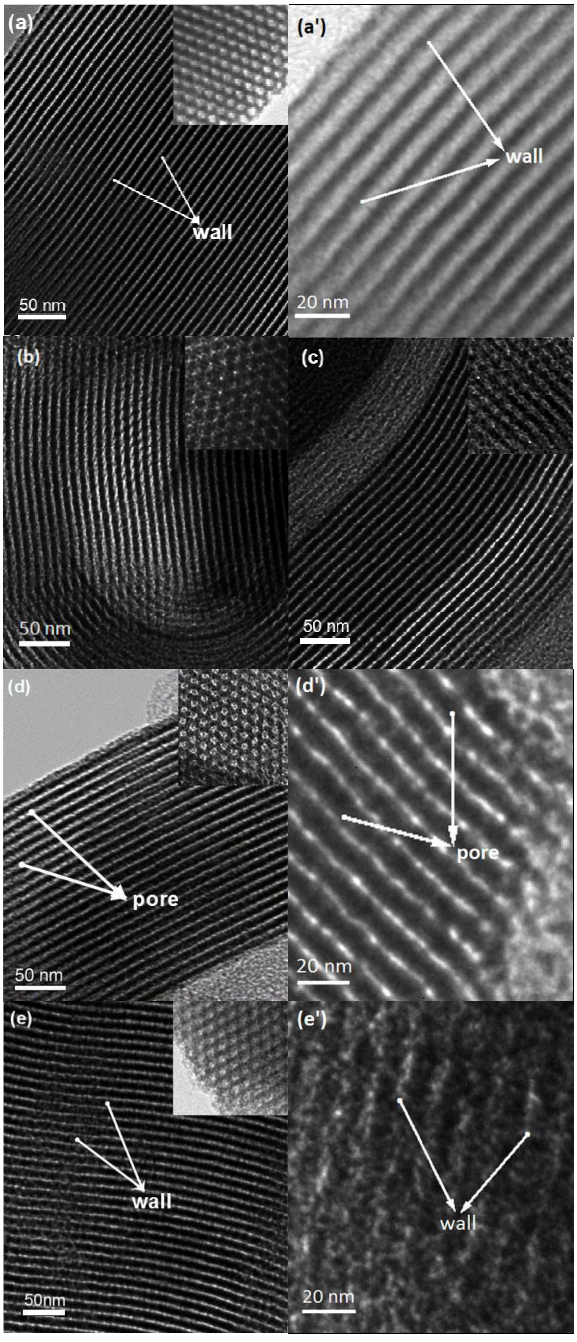

Fig. 6 TEM images of (a) SBA-15, (a') SBA-15-stained, (b) SBA-**Bp**-10, (c) SBA-**Np**-10, (d) SBA-**Am**-10, (d') SBA-**Am**-10-stained, (e) SBA-**T**-10, (e') SBA-**T**-10-stained.

3.8 Determination of the location aminopropyl groups by condensation the amino-functionalized materials with benzaldehyde

To further verify the location of amino groups of materials made from different methods (SBA-**T**-10 and SBA-**Am**-10), benzaldehyde(**A**) was used to form imine with amino groups in the materials (Scheme 2). If amino groups locate at the pore surface of the nesosilicates, the introduction of **A** into the pore by formation of imine with amino groups on the pore surface would reduce the pore size, or otherwise, the pore size would be remained unchangeable.

The mesoporous properties of SBA-**T**-10 and SBA-**Am**-10 before and after **A** treatment obtained by nitrogen adsorption experiments, are presented in Table 3. It is interesting that the pore size of SBA-**T**-10 had reduced slightly from 5.58 to 5.47 nm, while BET surface and pore volume of SBA-**T**-10 did not change significantly after treatment of **A**. In contrast, the pore size of SBA-**Am**-10 had been reduced from 6.58 to 5.78 nm, and pore volume from 0.941 to 0.773 cc/g. These could be explained by the different location of amino groups in SAB-**T**-10 and SBA-**Am**-10. Since a **TEOS** pre-hydrolysis process was used for synthesis of SBA-T-10, in which amino groups were distributed both in the pore channels (minor) and inside the walls of the resulting materials, little **A** could be attached on pore surface. The changes in pore size, BET surface and pore volume are ignorable. On the other hand, amino groups are mostly located on the pore surface of SBA-**Am**-10, they are available to react with **A**, resulting in pore size and pore volume changes. These results are in consistent with what observed in TEM stain images.

3.9 Kinetic study of flavanone synthesis

Amino-functionalized SBA-15 type material prepared by TEOS pre-hydrolysis method, has been found to be an effective base catalyst for the synthesis of flavanone(**Fl**).[22,28,29] Xueguang Wang et al. found that the yield of **Fl** from and 2'-hydroxyacetophenone(**B**) catalyzed by amino functionalized SBA-15 was the highest under solvent free condition, and DMSO was the best solvent for the reaction. For operative purpose, we use DMSO as solvent to study the kinetic behavior of the reaction catalyzed by two types of functionalized mesoporous materials. Two materials SBA-**Am**-10 and SBA-**T**-10 had comparable loading of amine groups, based on the elementary analysis (Table I), were chosen to catalyze the reaction of **A** and **B** (Scheme 3). The kinetic behaviors of the reaction were monitored by HPLC analysis.

The total yield of **Fl** catalysed by SBA-Am-10 was about 20%

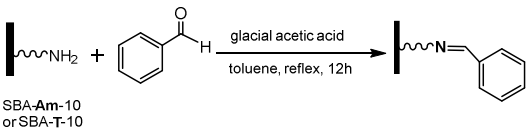

Scheme 2 Condensation reaction of the amine function with **A**.

Table 3 Texture properties of materials obtained with two methods after treated with **A**

Samples	Before reaction			After reaction		
	Pore size (nm)	BET surface (m^2/g)	Pore volume (cc/g)	Pore size (nm)	BET surface (m^2/g)	Pore volume (cc/g)
SBA-**T**-10	5.58	545.6	0.761	5.47	539.8	0.735
SBA-**Am**-10	6.58	571.6	0.941	5.78	550.8	0.773

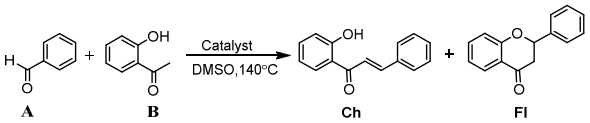

Scheme 3 synthesis of **Ch** and **Fl** catalysed by amino-functionalized mesoporous silicates.

higher than that of SBA-**T**-10 (Fig. 7 and Table 4). It was also about 2 h faster to reach the highest volume of yield (Fig. 7).The results could be interpreted as amino groups of SBA-**Am**-10 are more accessible than those of SBA-**T**-10 for the catalytical synthesis of **Fl** from **A** and **B**.

Since two steps were involved in the synthesis of **Fl** from Claisen-Schmidt condensation of **A** and **B**, followed by cyclization of **Ch** to **Fl**. To investigate the catalytic performance of the materials, we checked the cyclization of **Ch** in the presence and absence of catalyst and solvent (Scheme 4). The conversion of **Ch** in the presence of catalysts, DMSO and no solvent and without materials at 140 ℃ for 4 h are shown in Table 5.

As can been seen from Fig. 8, the two curves are almost overlapped, indicating that both of the materials were efficient

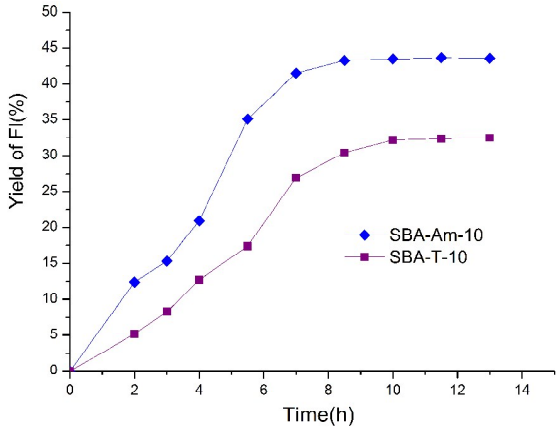

Fig. 7 Kinetic curves of yield of **Fl** from Claisen-Schmidt condensation of **A** and **B** catalyzed by SBA-**Am**-10 and SBA-**T**-10, respectively.

Table 4 The catalytic performance of materials in the condensation of **A** and **B** with DMSO at 140 °C for 8 h [a]

Entry	Catalyst	Conversion of **A** (%)	Yield of **Fl** [b] (%)
1	SBA-Am-10	69	44
2	SBA-T-10	53	33
3	SBA-15	<5	<3
4	--	--	--

[a] Reaction conditions: 6 mmol **A**; 4 mmol **B**; 2 ml DMSO; 0.25g SBA-15,SBA-**T**-10 or SBA-**Am**-10. [b] The yield of **Fl** were analyzed by HPLC.

in terms of converting **Ch** into **Fl**. In other words, the cyclization does not related with the distribution of amino groups in the materials.

To verify if the mesopores were responsible for the cyclization, blank SBA-15 with/without DMSO were used for the same reaction. The selectivity to **Fl** were also similar with those of amino functionalized materials. Surprisingly, when no solid catalyst was added in DMSO solution of **Ch**, the selectivity of **Fl** was also 66%. When **Ch** alone was heated to 140 °C for 4h, only 9% of **Fl** was detected. The results revealed that DMSO, amino-functionalized SBA-15 and none functionalized SBA-15 can catalyze the cyclization of **Ch**. Comparing data in Table 4 and Table 5, we could conclude that amino-functionalized SBA-15 was an effective catalyst for the Claisen-Schmidt

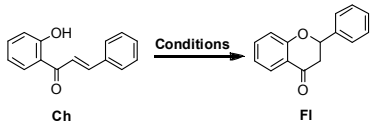

Scheme 4 Reaction of **Ch**.

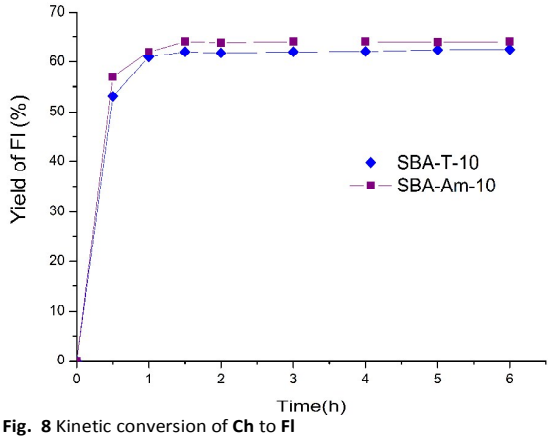

Fig. 8 Kinetic conversion of **Ch** to **Fl**

Table 5 Cyclization of **Ch** over 20mg materials or without materials at 140 ℃ for 4 h

Entry	Solvent	Catalyst	Yield of **Fl** (%)
1	DMSO	SBA-**Am**-10	64[a]
2	--	SBA-**Am**-10	70[b]
3	DMSO	SBA-**T**-10	62[a]
4	--	SBA-**T**-10	71[b]
5	DMSO	SBA-15	69[a]
6	--	SBA-15	61[b]
7	DMSO	--	66[c]
8	--	--	9[d]

[a] The yield of Fl were analyzed by NMR. Reaction conditions: 0.036mmol Ch, 2mL DMSO. [b] free-solvent. [c] without materials. [d] solvent-free and without materials.

condensation. Mesoporous silicats made with aryl-protecting groups method are more efficient for Claisen-Schmidt condensation than that of conventional **TEOS** prehydrolysis method.

Conclusions

The synthetic method for hexagonally ordered mesoporous silicates with amino groups functionalized on the pore channels was developed by a aromatic protecting group approach. Four aromatic groups were used and was founded that the soluibility and hydrophobosity of the aromatic groups affected the ordering of the resulted materials. The most critical difference between SBA-**Am**-10 and SBA-**T**-10 was the distribution of amino groups integrated in the materials, based on TEM and **A** condensation Experiments. The advantage of the materials in catalysis of **Fl** synthesis were compared with materials made by TEOS prehydrolysis method. Fast and higher yield of **Fl** was obtained by SBA-**Am**-10 catalyzed Claisen-Schmidt condensation from **A** and **B**. Further investigation of the mesoporous silicates on other reactions are under way in our laboratory.

Acknowledgements

This work was financially supported by National Natural Science Foundation of China (NSFC 21442012 and NSFC 21372213).

Notes and references

1 T. Yokoi, H. Yoshitake, T. Yamada, Y. Kubota and T. Tatsumi, *J. Mater. Chem.*, 2006, **16**, 1125.
2 Y. Xia and R. Mokaya, *Angew. Chem. Int. Ed*., 2003, **42**, 2639.
3 J. Mdoe, J. H. Clark and D. J. Macquarrie., *Synlett*, 1998, **6**, 625.
4 L. Martins, W. Hölderich, P. Hammer and D. Cardoso, *J. Catal.*, 2010, **271**, 170.
5 T. M. Suzuki, T. Nakamura, K. Fukumoto, M. Yamamoto, Y. Akimoto and K. Yano, *J. Mol. Catal. A: Chem.*, 2008, **280**, 224.
6 A. C. Blanc, D. J. Macquarrie, S. Valle, G. Renard, C. R. Quinnb and D. Brunela, *Green Chem*., 2000, **2**, 283.
7 A. S. M. Chong and X. S. Zhao, *Catal. Today*, 2004, **93-95**, 293.
8 D. J. Macquarrie and D. B. Jackson, *Chem. Commum.*, 1997, 1781.
9 M. J. Climent, A. Corma, S. Iborra and J. Primo, *J. Catal.*, 1995, **151**, 60.
10 A. Corma, *Chem. Rev.*, 1997, **97**, 2373.
11 F. Goettmann and C. Sanchez, *J. Mater. Chem.*, 2007, **17**, 24.
12 Q. Wei, Z. R. Nie, Y. L. Hao, L. Liu, Z. X. Chen and J. X. Zhou, *J. Sol-gel Sci Tech*., 2006, **39**, 103.
13 A. S. M. Chong, X. S. Zhao, A. T. Kustedjo and S. Z. Qiao, *Micropor. Mesopor. Mater.*, 2004, **72**, 33.
14 R. Sanz, G. Calleja, A. Arencibia, E. S. Sanz-Pérez, *Micropor. Mesopor. Mater.*, 2012, **158**, 309.
15 C. Yu, B. Tian, J. Fan, G. D. Stucky and D. Zhao, *Chem. Commun.***2001**, 2726.
16 G. T. Luo, Y. P. Li, A. Wang, Q. Lin, G. L. Zhang and C. Wang, *Open Chemistry*, 2015, **13**, 756.
17 C. M. Yang, B. Zibrowius and F. Schüth, *Chem. Commun.* **2003**, 1772.
18 A. Mehdi, C. Reyé, S. Brandès, R. Guilard and R. J. P. Corriu, *New J. Chem.*, 2005, **29**, 965.
19 A. Patti, A. D. Mackie, V. Zelenak and F. R. Siperstein, *J. Mater. Chem*., 2009, **19**, 724.
20 J. E. Lofgreen, I. L. Moudrakovski and G. A. Ozin, *ACS Nano*, 2011, **5**, 2277.
21 N. T. S. Phan and C. W. Jones, *J. Mol. Catal. A: Chem.*, 2006, **253**, 123.
22 X. G. Wang, S. K. Kyle, J. C. C. Chan and S. Cheng, J. *Phys. Chem. B*, 2005, **109**, 1763.
23 C. T. Kresge, M. E. Leonowicz, W. J. Roth, J. C. Vartuli and J. S. Beck, *Nature*, 1992, **359**, 710.
24 G. S. Attard, J. C. Glyde and C. G. Göltner, *Nature*, 1995, **378**, 366.
25 D. Y. Zhao, Q. S. Huo, J. L. Feng, B. F. Chmelka and G. D. Stucky, *J. Am. Chem. Soc*., 1998, **120**, 6024.
26 Y. J. Gu and B. Yan, *Eur. J. Inorg. Chem*., 2013, 2963.
27 K. S. Sing, W. D. H. Everett, R. A. W. Haul, L. Moscou, R. A. Pierottli, J. Rouquérol and T. Siemieniewska, Pure & Appl. Chem., 1985, 57, 603.
28 X. G. Wang, J. C. C. Chan, Y. H. Tseng and S. Cheng, *Micropor. Mesopor. Mater.,* 2005, **85**, 241.
29 S. Y. Chen, C. Y. Huang, T. Yokoi, C. Y. Tang, S. J. Huang, J. J. Lee, J. C. C. Chan, T. Tatsumi and S. Cheng, *J. Mater. Chem.,* 2012, **22**, 2233.

Graphical Abstract

Synthesis of hexagonal mesoporous silicates with amino groups functionalized on the pore channels by a co-condensation approach

Yunping Li,[ab] Wei Xiong,[ab] Chun Wang,[a,*] Bo Song[ac] and Guolin Zhang[a]